**Journal of Magnetics** 15(4), 213-220 (2010) DOI: 10.4283/JMAG.2010.15.4.213

# Chopper Application for Magnetic Stimulation

**Sun-Seob Choi[1], Sun-min Lee[2], Jun-Hyoung Kim[3], and Whi-Young Kim[4]***

[1]*Department of Radiology/Neuro Radiology Section, Dong-A University Medical Center, Busan 602-715, Korea*
[2]*Department of Occupational Theraphy, Dong-ju College University, Busan 602-715, Korea*
[3]*Hye Kwang High School, Busan 600-081, Korea*
[4]*Department of Biomedical Engineering, Dong-ju College University, Busan 602-715, Korea*

(Received 1 September 2010, Received in final form 21 October 2010, Accepted 21 October 2010)

**Since the hypothalamus immediately reacts to a nerve by processing all the information from the human body and the external stimulus being conducted, it performs a significant role in internal secretion; thus, a diverse and rapid stimulus pulse is required. By detecting Zero Detector accurately via the application of AVR on-Chip (ATMEL) using commercial electricity, chopping generates a stimulus pulse to the brain using an IGBT gate to designate a new magnetic stimulation following treatment and diagnosis. To simplify and generate a diverse range of stimuli for the brain, chopping can be used as a free magnetic stimulator. Then, commercial frequency (60Hz) is chopped precisely at the first level of the leakage transformer to deliver an appropriate stimulus pulse towards the hypothalamus when necessary. Discharge becomes stable, and the chopping frequency and duty-ratio provide variety after authorizing a high-pressure chopping voltage at the second level of the magnetic stimulator. These methods have several aims. The first is to apply a variable stimulus pulse via accurate switching frequency control by a voltaic pulse or a pulse repetition rate, according to the diagnostic purpose for a given hypothalamus. Consequently, the efficiency tends to increase. This experiment was conducted at a maximum of 210 W, a magnetic induced amplitude of 0.1~2.5 Tesla, a pulse duration of 200~350 $\mu$s, magnetic inducement of 5 Hz, stimulus frequency of 0.1~60 Hz, and a duration of stimulus train of 1~10 sec.**

**Keywords :** stimulus pulse, detecting zero detector, commercial frequency, duty-ratio, chopping

## 1. Introduction

A pulse magnetic field boosts the brain's tolerance to oxygen deficiency and lowers blood pressure to an average level by promoting nervous system function and by improving nitrogen and carbon in addition to decreased emotional tension [1-3]. It also advances the action ability of the endocrine system. Since the human body is a conductor, it can generate an induced current, which is able to stimulate muscles or nervous cells. It is possible to cure each part that could not be treated by electrotherapy with non-invasive methods, and there is no skin damage due to the electrode [4-7]. Moreover, it is possible to obtain various treatment and diagnostic results because stimulating an internal part of the human body with deep stimulation is possible. Fig. 1 shows a diagram of the proposed magnetic stimulation device.

Existing magnetic stimulators supply charged energy into the condenser using an on/off of switching device attached to a stimulus coil through a pulse transformer after conversion to a high-pressure pulse using a capacity and pulse transformer [8-10]. The disadvantage is the capacity of condenser should be enlarged for rectifying sections that convert AC to DC and high-output. These problems can be controlled more easily and the efficiency will be improved if chopper frequency and duty-ratio increase using the effective chopping of volt-ampere through an exchange chopper method during the periodic section of plus (+) and minus (−) than the using the DC discharge method.

To form a circuit using an SCR and TRAIC device for enlargement of chopper frequency and duty-ratio of the exchange chopper, an assistant power device is required for arc extinguishing; however, a power device for accurate arc extinguishing is difficult to compute and it typically has flaws not because it is a complicated circuit but because of the circuit's response characteristic [11, 12]. Nevertheless, the use of an insulated gate bipolar transistor (IGBT) provides a higher circuit operating frequency and a much

*Corresponding author: Tel: +82-51-200-3449
Fax: +82-51-200-3235, e-mail: ndyag@dongju.ac.kr

ⓒ 2010 Journal of Magnetics

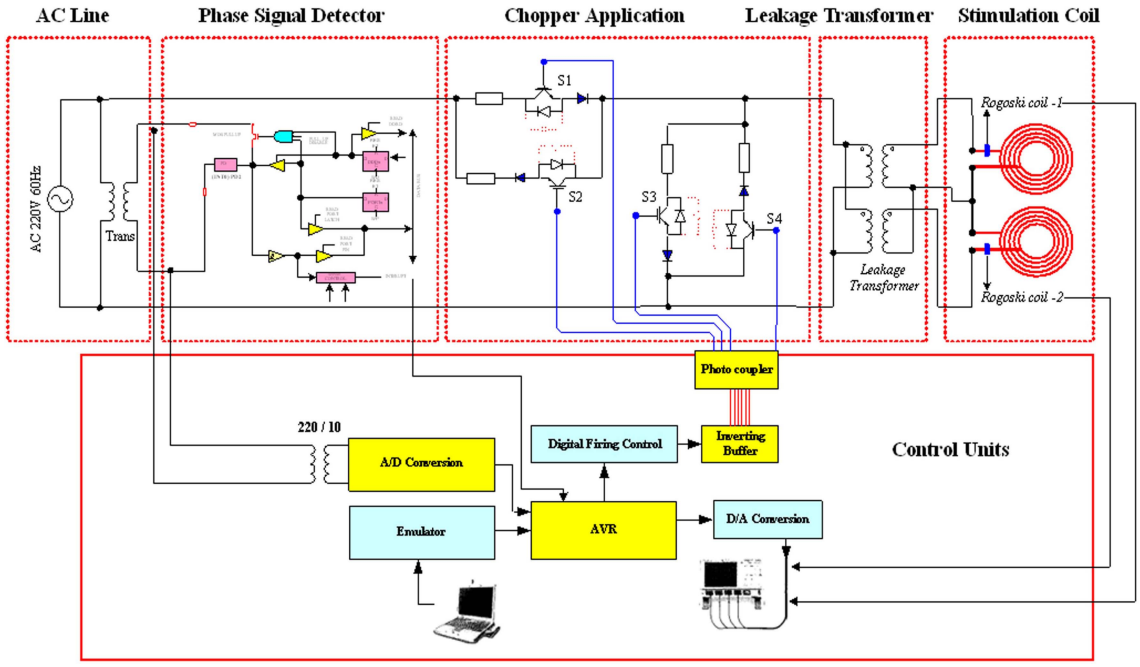


**Fig. 1.** Diagram of the proposed magnetic stimulation device.

faster response characteristic, because it is able to fulfill a pulse period of the control circuit as it is to operation frequency of IGBT as well as the original operation frequency IGBT has is much higher than SCR or TRIAC [13, 14]. Therefore, this study accurately detects the frequency of commercial electricity by using the Zero Detector function of AVR on-chip (ATMEL) and drives diversely according to the phase of the IGBT gate. Next, a high-pressure chopping voltage is authorized to the second level of the magnetic stimulator with a detailed chopping on a commercial frequency (60 Hz) at the first level of the leakage transformer. A physiological signal obtained by EEG or ECG spectrum frequency is handled with an RC interphase, and several experiment results, such as image processing, are organized.

## 2. Design

The whole system is formed with from an AC-Line, phase signal detector, chopper application, leakage transformer, control unit, and stimulation coil unit in Fig. 1. According to the Faraday-Henry law, method (1) is the same as connecting to a closed circuit with variable magnetic flux, $F$.

$$\wp = -\frac{dF}{dt} \tag{1}$$

$\wp$ is electromotive force (emf), $F$ is magnetic flux [Wb], and $t$ is time. Flow velocity is due to coil current ($I$). Flow velocity, $F=LI$, where $L$ represents inductance of the coil and emf can be used as seen in Eq. (2).

$$\wp = -\frac{dF}{dt} = -L\frac{dl}{dt} \tag{2}$$

Here, $L$ indicates the inductance of the coil [$H=Wb/A=Vs/A$], and $I$ is the current inside the coil [$A$]. Inductance from a flat multiple-layer disk coil is determined using Eq. (3).

$$L \approx \mu N^2 \frac{\pi\gamma^2}{0.8\gamma + 1.1\zeta} \tag{3}$$

The first layer is a copper pipe (2.5 mm, 10 turns, physical level $r$ = 14~36 mm); it is attached to a standard, measured impedance coil of 10 m with an inductance of 9.67 [H], where $L$ = inductance of coil [H], $\mu$ = permeability of the coil core [Vs/Am], N is the number of turns on the coil, $R$ is the coil radius [m], $l$ is the coil length [m], and $s$ is the coil width [m]. This is charged by 90~260 V and is discharged through a stimulus coil with four banks of power devices. The requirements to stimulate energy structures are proportional to the square of the magnetic field. According to the inducement method of Faraday, this magnetic field is nearly directly proportional to the size of the magnetic field and to pulse duration.

$$W \infty B^2 \infty E^2 t^2 \tag{4}$$

$W$ is the energy required to stimulate a fiber, $B$ is the density of the flow velocity in a magnetic field, $E$ is the

electric field, and $t$ is the pulse duration.

$$E \infty \frac{\sqrt{W}}{t} \tag{5}$$

This indicates that the transmembrane voltage, $Vm$, satisfies the equation.

$$\lambda^2 \frac{\partial^2 V_m}{\partial \pi^2} - V_m = \tau \frac{\partial V_m}{\partial_t} + \lambda^2 \frac{\partial E_x}{\partial x} \tag{6}$$

Where $V_m$ is the transmembrane voltage, $x$ is the orientation of the fiber. $E_x$ is the $x$-component of the magnetically induced electric field (proportional to the $x$-component of the induced current density). In this study the AC-Line uses power coming through commercial electricity without any rectifying action. In Fig. 2, phase signal detector attempts to generate diverse output values following loading condition by using a roll call in conjunction with phase after operating a zero detect with an one-chip-Microprocessor (ATMEL). Characteristically, the AVR chip contains 130 Powerful Instructions as low electric consuming AVR 8-bit Microcontroller with high reliability and Nonvolatile Program and Data Memories by a single-chip, two-cycle multiplier. In addition, it is a self-programming, in-system, programmable flash memory. In addition, it is a self-programming, in-system, programmable Flash memory. In addition, two 8-bit timers/counters with separate pre-scaler and compare modes, one 16-bit timer/counter with separate pre-scaler, compare mode, and capture mode are used. There are external and internal interrupt sources, and the AT90s8535 has an operating voltage of 2.7~5.5V with speed grades of 0~8 MHz. A chopper application, used as an exchange chopper controller coupled with an electricity-using switching controller can be formed with several power devices to drive the system. Essentially, it has four switches and is compatible with a current single-phase chopper. It is driven by a gate signal created on four traditional switches, and it uses a key-pad to enter commands and display on the other AVR-2. Fig. 3 shows (a) port D, and (b) Port B. Port D presents an inner pull-up register, both sides of the I/O port, and an eight beat. The output buffer is 20 mA. From the entry, D pins provide a low source of electricity if pull-up resistance activates, and Port D provides various special functions of AT90s8535. Therefore, a chopper helps the output velocity to adjust the duty-ratio of the chopping pulse over a spectrum of values. Entered velocity is indicated in Eq. (8), where $W$ is the angular frequency and $V_m$ is the velocity magnitude.

$$V_m = V_m \cos(wt) \tag{8}$$

Chopper output voltage can be expressed as in Eq. (9).

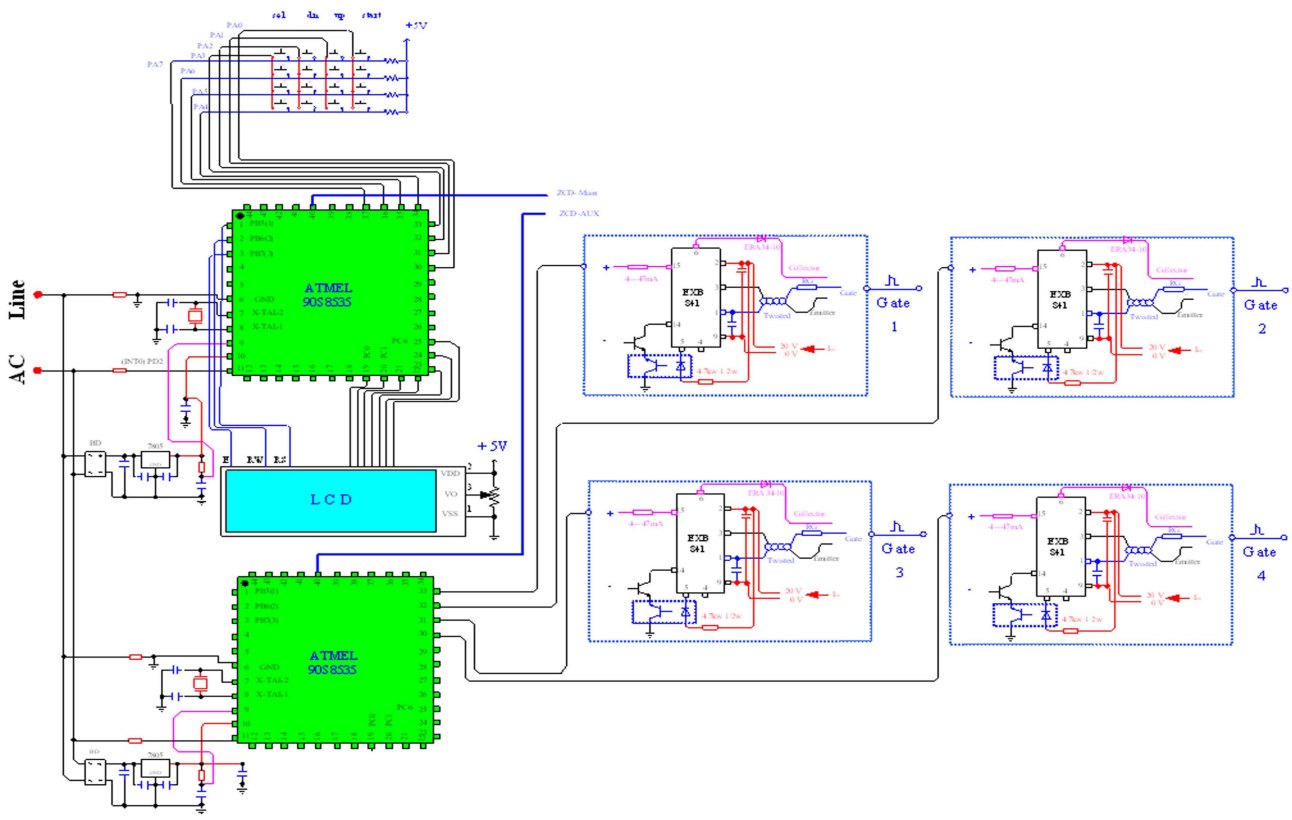


**Fig. 2.** AVR single-chip control and drive circuit.

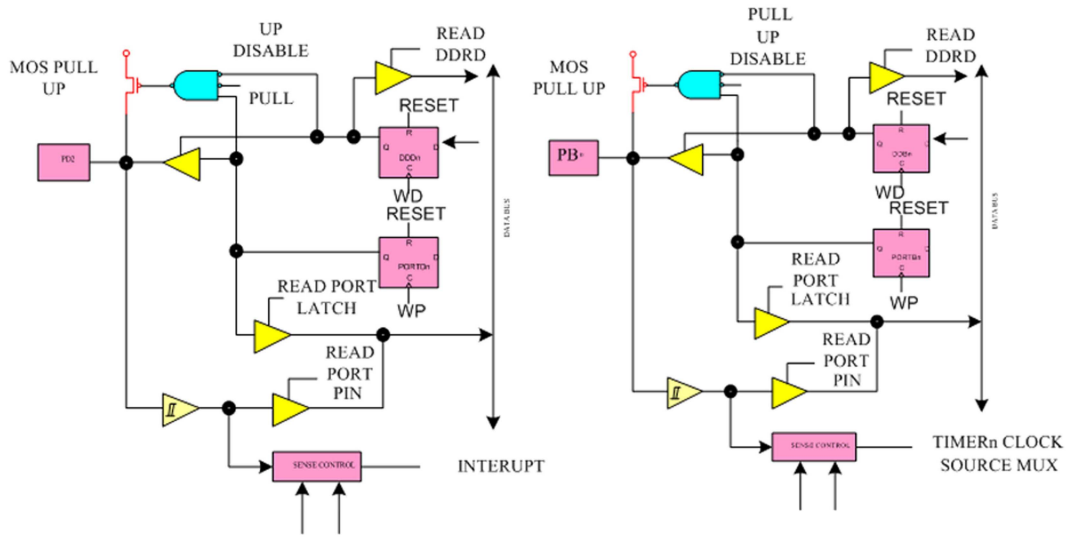


**Fig. 3.** AVR single-chip 90S8535, port D, and port B.

$$Vc_m = DV_{mM}\cos(wt) + \sum_{K=1}^{\infty} \frac{V_m \sin KD\pi}{K\pi}\cos(K\omega S \pm \omega)t \quad (9)$$

Both $D$ and $\omega S$ show duty-ratio and each frequency. Equation (9) describes a switching frequency that contains a basic component and a harmonic. An output voltage-filtered, exchange chopper in the standard configuration can be described by Eq. (10).

$$Vo = DV_{mM}\cos(wt - \varphi) \quad (10)$$

$\varphi$ represents the basic phase delay caused by the filter. It will be controlled much easily and the efficiency will be improved if the voltage chopping of the exchange copper method is used effectively during the periodic section of plus (+) and minus (–), thus increasing the chopper frequency and duty-ratio. To increase the chopper frequency and duty-ratio, IGBT will be used to achieve the pulse frequency of the control circuit as it operates at the IGBT frequency. Alternatively, the IGBT operating frequency can become the circuit operating frequency, and it tends to respond much faster. $D_1$ is being chopped when the AC 220 V during the operation of chopper circuit is positive. At this point, power is supplied, simultaneously $S_3$ is on and $S_4$ is off, and the Free-Wheeling Pass is approached to continue the load current.

Conversely, $S_2$ is on, $S_3$ is off, and $S_4$ is on when it is negative. The diode connected in parallel each switching device is used to protect switching devices. The leakage transformer copes with the changes of chopping frequency and duty-ratio under conditions in which a stable discharge is maintained by chopping with a commercial frequency (60 Hz) at the first level and by authorizing the chopping voltage of high-pressure on the magnetic stimulator of the second level. The control unit determines the driving pulse, which drives S2, S2, S3, S4, and the display using AR90S8535 (ATMEL). AVR (ATMEL90S8535) supplies the delay, superposition, and various pulses through each pulse towards EXB841 (FUJI) of the IGBT private driving module via a keypad. This experiment uses an 8 mm inner diameter, 10 mm outer diameter coil at Stimulation coil , and it can withstand a voltage of 1,500 V. It has a width (t) of 0.2 mm, and it is made with glass fiber, the material used to prevent interference and obstacles along a wire. During the second phase for complete shielding, a withstanding voltage of 5,000 W and a width (t) of 0.2 mm are used. In addition, heat treatment (temper) is performed at 650°C for 10 minutes (the entire treatment, with 5 minutes for the final stage); this process reinforces materials for various uses. A large, helical coil was produced using Litz wire (280 strands). The coil consisted of 10 turns with a diameter of 150 mm. The inductance value of this coil was approximately 9 $\mu$H, and the maximum strength of the magnetic field was 1.2 Tesla. The stimulation coil designed and built primarily to treat wide parts, such as the shoulder, back, stomach, etc.

A small, helical coil probe was built using Litz wire (180 strands). The coil probe consisted of 10 turns and a diameter of 100 mm. The inductance value of this coil was 9 $\mu$H, and the maximum strength of the magnetic field was 2.2 Tesla. The stimulation coil is preferred for use on narrow parts, such as the neck, elbow, and ankle or on infants. A figure-eight coil probe was produced by connecting two helical coils with Litz wire (150 strands). The figure-eight coil consisted of 10 turns and a diameter of 80 mm. The inductance value of this coil was approximately 9 $\mu$H, and the maximum strength of the magnetic

field was 1.2 Tesla. This stimulation coil could be used to focus treatment to the head or specific areas. The stimulation coil had a magnetic field strength of 2 T; an electric field of 400 V/m; an induced current density per phase of 14 mA/cm$^2$/ph; an induced charged density per phase of 0.85 $\mu$C/cm$^2$/ph; and an energy deposited per phase of 3.0 $\mu$F/cm$^3$. Chopper units are designed to be able to vary the output magnetic stimulation by changing the regular pulse width and duty-ratio.

A switching device is used with the proper IGBT to switch kHz, and it also is used with current resistance limits to protect switching power. Although the duty-ratio is adjustable from 10 to 95 percent, the duty-ratio is adjusted 65~94% of the maintenance voltage to maintain a stable discharge of the initial discharge voltage inside the magnetic coil. Moreover, the pulse width is designed to adjust from 10.11 $\mu$s to 668.7 $\mu$s.

## 3. Experiment Results

From this study reports various characteristics of each designed component (AC-Line, phase signal detector, chopper application, leakage transformer, control unit, and chopper-applied magnetic stimulation of the coil unit. Table 1 shows the number of pulses authorized to AVR and the IGBT trigger component. Fig. 4 presents the ratio of input to output signal of the zero detect circuit and the IGBT trigger according to the frequency as well as the voltage waveform of the first level of the transformer. Fig. 5 indicates the output waveform coming from the PBO 40 terminal of the AVR chip (AT90S8535). The upper waveform at the commercial power (60 Hz) status shows the exchange radio waveform (Fig. 6); the middle

**Table 1.** The number of pulses authorized to AVR and the IGBT trigger component.

| Frequency | The number of pulse authorized to AVR by ZCS | The number of pulse authorized to IGBT trigger part by AVR |
|---|---|---|
| 5 Hz | 24 | 1 |
| 10 Hz | 12 | 1 |
| 20 Hz | 6 | 1 |
| 30 Hz | 4 | 1 |
| 40 Hz | 3 | 1 |
| 60 Hz | 2 | 1 |

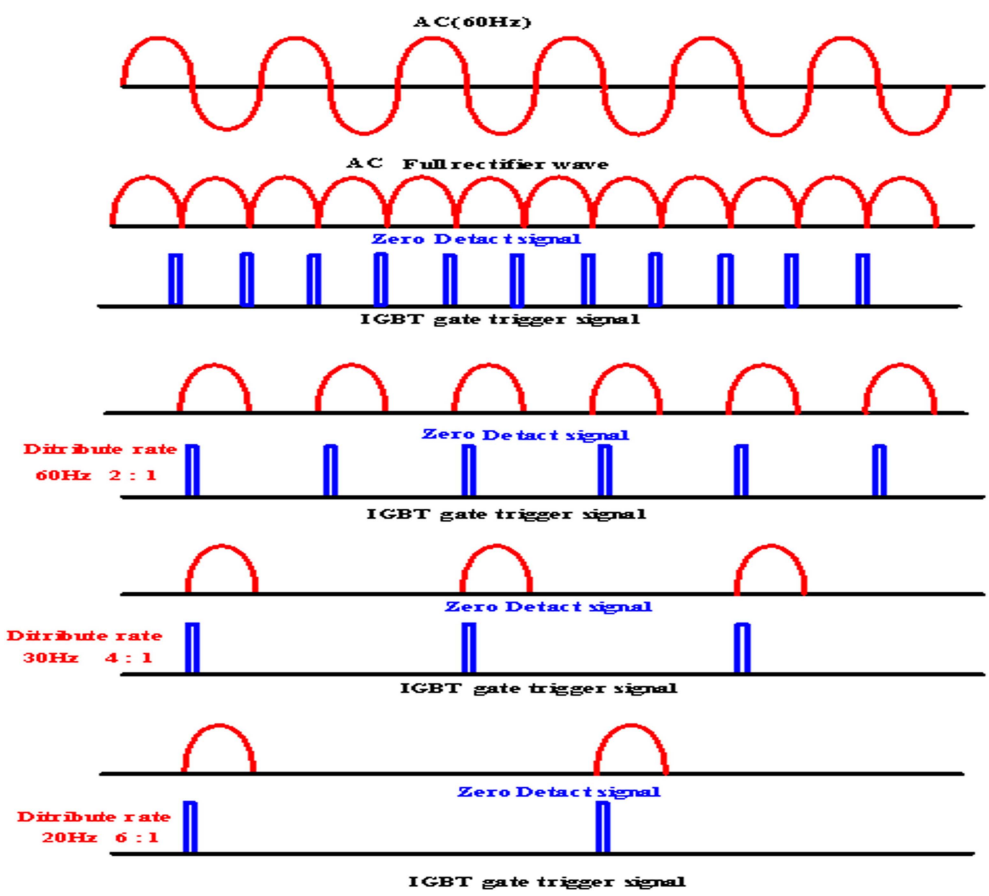


**Fig. 4.** The waveform of the zero detector input-output signal and the IGBT trigger signal at working frequency.

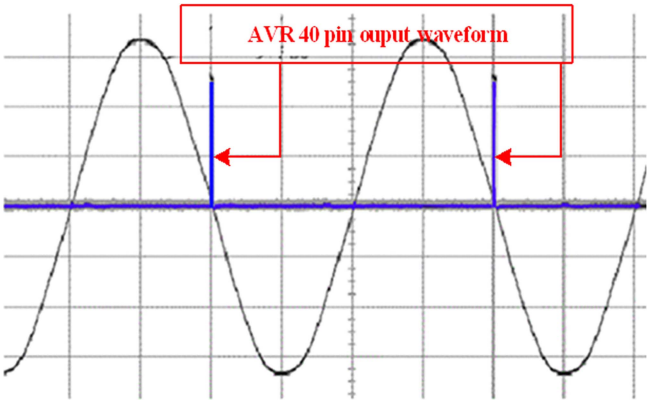


**Fig. 5.** Main Input and PBO Output (AT90S8535).

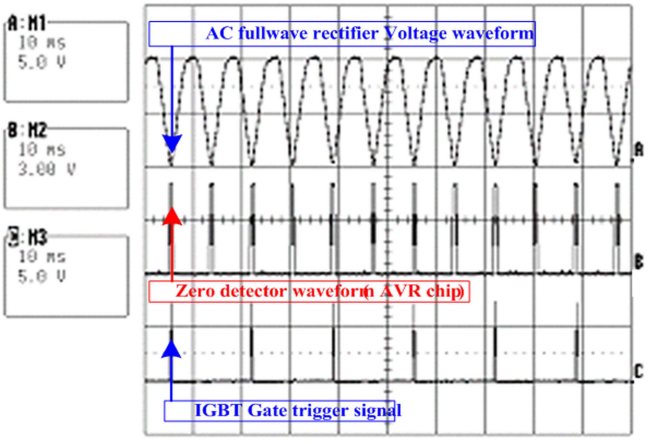


**Fig. 6.** Waveform of the input-output signal in the ZCS and IGBT trigger circuit (60 Hz).

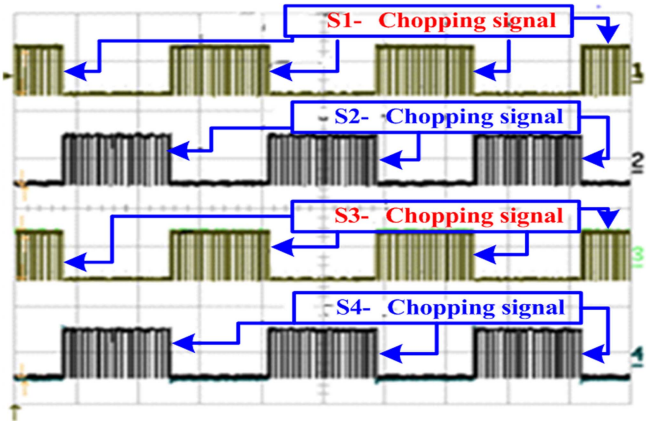


**Fig. 7.** Waveform of the driving signals in difference mode.

panel indicates the output waveform from the 40 pin of the AVR chip, and the bottom waveform demonstrates the driving waveform of the IGBT. $S_1$ tends to chop when AC220V is positive due to the operation of the chopper circuit (Fig. 7). Power is supplied, and simultaneously the

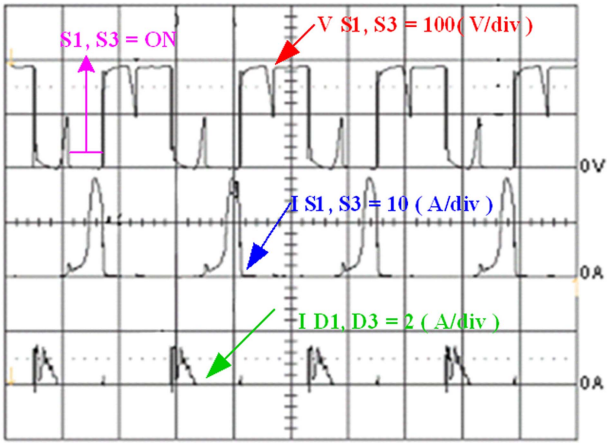


**Fig. 8.** Experimental waveforms for the collector-to-emitter voltage, current of IGBT, S1, S3, and bypass current flowing through diodes D1 and D3.

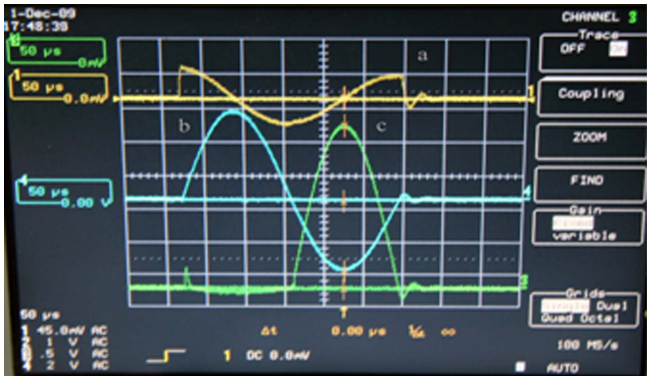


**Fig. 9.** Discharge waveform, capacitor discharge, and stimulation coil current waveform.

load current continues approaching the free-wheeling pass when $S_3$ is on and $S_4$ is off.

Conversely, the driving waveform produced when $S_2$ is on, $S_3$ is off, and $S_4$ is on is negative. Fig. 8 shows the experimental waveforms for the collector-to-emitter voltage, IGBT current, S1, S3, and bypass current flowing through diodes D1 and D3. Each current and voltage show a current waveform measured by the Lecroy high voltage probe (Probe X 6000V) and the Rogoski current waveform transducer, CWT (Fig. 9). Since the initial discharge voltage, *Vi*, was 1000V and the complete discharge voltage, *Ve*, was 760 in this experiment, it was possible to obtain current loss capacity. It was possible to charge to the initial discharge voltage (*Vi*) of 1000 V within 20 mS after completing discharge, and a 50 Hz magnetic frequency could be realized when $v_{ini}$ was 1000 V. When the initial discharge voltage was 1000 V, a time-varying magnetic field of I Tesla occured 50 mm from the stimulated coil. Fig. 10 shows the experimental value of the mag-

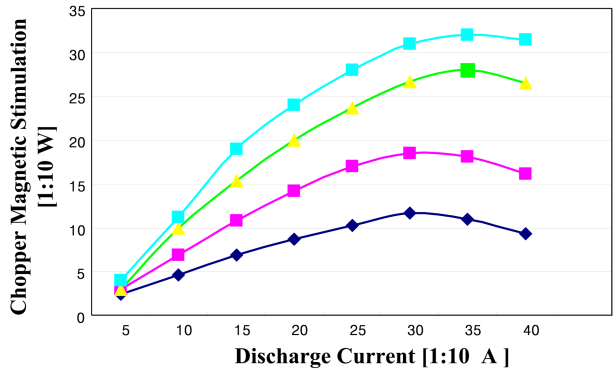


**Fig. 10.** Discharge current characteristic according to the maximum discharge at Chopper magnetic stimulation.

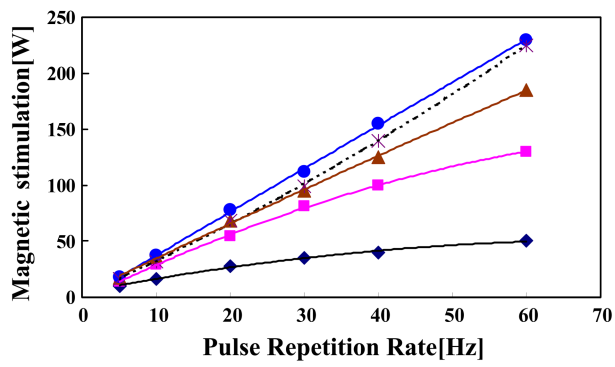


**Fig. 11.** Output characteristic of repetition rate following the maximum discharge at Chopper magnetic stimulation.

netic stimulation output from commercial frequency exchange discharge using a leakage transformer. Fig. 11 indicates the output of the magnetic stimulator for the repetition rate. The average of the duty-ratio was determined from several experiments conducted under regular conditions; 210 W of output could be obtained when the duty-ratio was 92%. At 333.4 $\mu$s the off time provided a minimum 20 $\mu$s delay time due to the characteristics of the IGBT 1MBH60-100 used in this experiment. As the duty-ratio increased, the output of the magnetic stimulator also linearly increased. In magnetic stimulation, the ability of the discharge to stabilize and to remain stable is very important. The non-glutinous cooling of the magnetic stimulation is also significant. Liquid should be ideally circulated through the proper arrangement of a liquid flow and ventilator or a heat switchboard. By using ring blow, the circulation is better handled inside the magnetic coil. The ring blow used was at 232.4 torr (maximum pressure) and 5 $m^3$/min maximum air flow. When the ring blow was used in the experiment, a 5W higher output occurred and the stability was effected considerably.

## 4. Conclusion

To deliver the proper magnetic pulse to the hypothalamus using a free magnetic stimulator with chopping after detecting an accurate zero detector with the application of a AVR one-Chip to commercial electricity, a detailed chopping was operated for commercial frequency (60 Hz) at the first level of leakage transformer, and it was examined by investigating the change of chopping frequency and duty-ratio. The method reduces load sharing, input energy, and transformer load sharing of the exact magnetic pulse and magnetic coil length for the hypothalamus; moreover, the efficiency also increases. Other than a general magnetic stimulation power supply, current installation is simple and convenient without using a filter capacitor section. In addition, changing energy density is varied with the duty-ratio by controlling the AC line directly with switching device (*i.e.* it did not control the output by changing the magnetic stimulation current according to the energy per existing pulse.

Current pulse width as well as pulse repetition rate of the magnetic stimulator output could be controlled by switching the frequency control according to power density, and the characteristic experiment is suitable for diagnostic purposes. Following the pulse duty-ratio control method, which drives the IGBT gate maximum magnetic frequency from low frequency to high frequency, the efficiency could be confirmed.

Because the magnetic stimulator is suitable for various applications, an output capacity 210 W was obtained by confirming the operating characteristics of the prototype. Based on the analysis of PC and an interface by data-mining method after measuring physiological signal separated by EEG, an ECG spectrum frequency (obtained after a stimulus pulse) a GUI was used to indicate (after image processing) the central nervous system.

## Acknowledgement

This work was supported by the Dong-A University Research Fund.

## References

[1] V. Walsh and M. Rushworth, Neuropsychologia **37**, 125 (1999).

[2] M. Van Asselen, R. P. C. Kessels, S. F. W. Neggers, L. J. Kappelle, C. J. M. Frijns, and A. Postma, Neuropsychologia **44**, 1185 (2006).

[3] M. S. George, Z. Nahas, F. A. Kozel *et al.*, CNS Spectrums **8**, 496 (2003).

[4] Atsushi Chiba, Masahiko Sendoh, Kazushi Ishiyama, Ken Ichi Arai, Hironao Kawano, Akio Uchiyama, and Hironobu Takizawa, J. Magnetics **12**, 89 (2007).
[5] H. Théoret, M. Kobayashi, A. Valero-Cabré, and A. Pascual-Leone, Supplements to Clinical Neurophysiology **56**, 211 (2003).
[6] T. C. Britton, B. U. Meyer, J. Herdmann, and R. Benecke, Muscle Nerve **13**, 396 (1990).
[7] S. Bae, Y.-K. Hong, J.-J. Lee, G. Abo, J. Jalli, A. Lyle, H. Han, and W. Gregory, J. Magnetics **13**, 37 (2008).
[8] M. Seyal, T. Ro, and R. Rafal, Neurol. **38**, 264 (1995).
[9] M. B. Miller *et al*., Neuroreport **7**, 1740 (1996).
[10] L. G. Cohen, B. J. Roth, J. Nilsson, N. Dang, M. Panizza, S. Bandinelli, W. Friauf, and M. Hallett, Electroencephalogr. Clin. Neurophysiol. **75**, 350 (1990).
[11] K. P. Esselle and M. A. Stuchly, IEEE Trans. Biomed. Eng. **39**, 693 (1992).
[12] B. W. Wilson, K. Caputa, M. A. Stuchly, J. D. Saffer, K. C. Davis, C. E. Washam, L. G. Washam, G. R. Washam, and M. A. Wilson, Bioelectromagnetics **15**, 563 (1994).
[13] S. Ueno, T. Tashiro, and K. Harada, J. Appl. Phys. **64**, 5862 (1988).
[14] S. J. Blakemore, D. M. Wolpert, and C. D. Frith, Neuroreport **11**, 11 (2000).